




Open Archive Toulouse Archive Ouverte (OATAO)

OATAO is an open access repository that collects the work of Toulouse researchers and makes it freely available over the web where possible

This is an author's version published in: <http://oatao.univ-toulouse.fr/21002>

Official URL: <https://doi.org/10.1002/pssb.201700261>

To cite this version:

Fedoseeva, Yuliya V. and Dubois, Marc and Flahaut, Emmanuel  and Vilkov, Oleg Yu and Chuvilin, Andrey and Asanov, Igor P. and Okotrub, Alexander V. and Bulusheva, Lyubov G. *Effect of Hydrogen Fluoride Addition and Synthesis Temperature on the Structure of Double-Walled Carbon Nanotubes Fluorinated by Molecular Fluorine.* (2018) physica status solidi b, 255 (1). 1700261. ISSN 0370-1972

Any correspondence concerning this service should be sent to the repository administrator: tech-oatao@listes-diff.inp-toulouse.fr

Effect of Hydrogen Fluoride Addition and Synthesis Temperature on the Structure of Double-Walled Carbon Nanotubes Fluorinated by Molecular Fluorine

Yuliya V. Fedoseeva,* Marc Dubois, Emmanuel Flahaut, Oleg Yu. Vilkov, Andrey Chuvilin, Igor P. Asanov, Alexander V. Okotrub, and Lyubov G. Bulusheva

Double-walled carbon nanotubes (DWCNTs) have been fluorinated by pure molecular fluorine (F_2) at room temperature or 200 °C and a mixture of F_2 with hydrogen fluoride (HF) at 200 °C that resulted in products with compositions of $CF_{0.12}$, $CF_{0.39}$, and $CF_{0.53}$ as determined by X-ray photoelectron spectroscopy. The differences in the structures of three kinds of fluorinated DWCNTs were revealed using transmission electron microscopy, Raman scattering, and near-edge X-ray absorption fine structure (NEXAFS) spectroscopy. Quantum-chemical modeling of the NEXAFS F K-edge spectra detected a change in the fluorine pattern with the increase of the F_2 treatment temperature. The presence of HF in fluorine gas was found to accelerate the fluorination process and cause a partial destruction of outer shells of the DWCNTs.

1. Introduction

Fluorinated carbon nanotubes (CNTs) attract the interest for electronic applications because of the possibility of energy gap tuning through sidewall chemical modification. Density functional theory (DFT) calculations have shown that depending on the fluorination pattern and the tube chirality, the bandgap in the fluorinated CNTs may vary from 2.7 to 0 eV.^[1] The different structures and hence properties of the fluorinated CNTs can be obtained by using various fluorination techniques.^[2,3] CNTs as well as graphite and graphene are usually fluorinated with the help of fluorine gas (F_2) at elevated temperatures.^[4–6] Fluorination tempera-

ture is one of the key parameters, which influence the composition and types of C–F bonding in the product.^[7,8] Note, that graphite does not interact with pure F_2 at ordinary conditions, while the process occurs with an admixture of hydrogen fluoride (HF) in the reacting gas.^[9,10] DFT calculations have revealed polarization of F_2 molecule when it forms a F_2 –HF complex.^[11] Thus, HF plays a catalytic role in the fluorination process by increasing the reactivity of F_2 . Zhang with co-authors have shown that in contrast to fluorination by atomic fluorine, fluorination by “pure” F_2 produces nonhomogeneous distribution of fluorine on the surface of single-walled CNTs (SWCNTs).^[2] Using DFT calculations, they demonstrated a chemisorption of HF molecules beside the fluorinated areas and concluded that HF influences the increase in the size of highly fluorinated regions, thus enhancing the fluorination inhomogeneity.

The questions about the destruction of CNT shells and fluorination of the inner tubes of double-walled CNTs (DWCNTs) and multi-walled CNTs (MWCNTs) during the fluorination procedure are still opened. With the help of high-resolution transmission electron microscopy (HRTEM), Raman spectroscopy, and X-ray photoelectron spectroscopy (XPS) data, Muramatsu with co-authors have revealed that fluorine atoms can be successfully attached to the outer shells of DWCNTs through the reaction with pure F_2 at 200 °C for 5 h, preserving the nanotube morphology.^[12] It has been demonstrated that in the fluorination process the outer surfaces of the DWCNTs are fluorinated and the inner shells remain intact.^[13,14]

Dr. Y. V. Fedoseeva, Dr. I. P. Asanov, Prof. A. V. Okotrub, Dr. L. G. Bulusheva
Nikolaev Institute of Inorganic Chemistry SB RAS
3 Acad. Lavrentiev Ave., 630090 Novosibirsk, Russia
E-mail: fedoseeva@niic.nsc.ru

Dr. Y. V. Fedoseeva, Dr. I. P. Asanov, Prof. A. V. Okotrub, Dr. L. G. Bulusheva
Novosibirsk State University
2 Pirogova Str., 630090 Novosibirsk, Russia

Prof. M. Dubois
Institut de Chimie de Clermont-Ferrand (ICCF)
Université Blaise Pascal, UMR CNRS 6296
24 Avenue Blaise Pascal, 63177 Aubière, France


Prof. M. Flahaut
Centre Interuniversitaire de Recherche et d'Ingénierie des Matériaux
Université Paul-Sabatier
Toulouse, France

Prof. E. Flahaut
CNRS, Institut Carnot Cirimat
F-31062 Toulouse, France

Dr. O. Yu. Vilkov
St. Petersburg State University,
1 Ulyanovskaya str., 198504 St. Petersburg, Russia

Prof. A. Chuvilin
CIC nanoGUNE Consolider
76 Tolosa Hiribidea, Donostia-San Sebastian 20018, Spain

Prof. A. Chuvilin
IKERBASQUE Basque Foundation for Science
3 Maria Diaz de Haro, Bilbao E-48013, Spain

 The ORCID identification number(s) for the author(s) of this article can be found under <https://doi.org/10.1002/pssb.201700261>.

DOI: 10.1002/pssb.201700261

In this paper, we used a DWCNT sample as a perfect model for the discovery of possible chemical modification of surface and interior space. Fluorination of DWCNTs was carried out by pure molecular fluorine at room temperature or 200 °C, and a mixture of F₂ with HF at 200 °C. HRTEM, Raman scattering, energy-variable XPS and near-edge X-ray absorption fine structure (NEXAFS) spectroscopy were used to reveal the changes in the composition and structure of DWCNTs fluorinated at these different conditions.

2. Experimental Section

2.1. Materials

DWCNTs were grown by catalytic chemical vapor deposition (CCVD) method using a mixture of methane (18 mol.%) and hydrogen at 1000 °C and a Mg_{1-x}Co_xO catalytic system^[15] and purified by heating in air at 450 °C for 1 h followed by treatment with concentrated HCl.^[16] The obtained sample consisted of *ca.* 80% DWCNTs, 20% SWCNTs, and a few triple-walled nanotubes. The outer diameter of the DWCNTs ranged from 1.2 to 3.2 nm, and the diameter of inner tubes varied from 0.5 to 2.5 nm.

Fluorination of DWCNTs was carried out under a pure F₂ gas flow at room temperature for 3 h (marked as sample RT) and at 200 °C for 2 h (marked as sample 200C). The mixture of F₂ and HF (less than 5%) produced by electrolysis of a KF · 2HF melt at 100 °C has been used for fluorination of DWCNTs at 200 °C for 10 min (marked as sample HF-200C).

2.2. Characterization

HRTEM images of fluorinated DWCNTs were collected on a JEOL-2010 microscope and a Titan 80–300 microscope. Raman spectra were measured on a LabRAM HR Evolution spectrometer using the 633-nm excitation from a HeNe laser. The NEXAFS and XPS experiments were performed at the Berliner Elektronenspeicher-Gesellschaft für Synchrotronstrahlung (BESSY II) using monochromatic radiation from the Russian-German beamline. NEXAFS spectra near the C K- and F K-edges were acquired in the total-electron yield mode with a typical probing depth of a few nanometers.^[17] The spectra were normalized to the primary photon current from a gold-covered grid. XPS C 1s spectra were measured at an excitation energy of 400 and 800 eV with a resolution of ≈ 0.07 and ≈ 0.1 eV (full width at half maximum, FWHM). XPS C 1s spectra were additionally recorded on a SpecsLab PHOIBOS 150 spectrometer with Al K α (1486.74 eV) excitation. The binding energies of the fluorinated samples were calibrated to the pristine DWCNT C 1s peak at 284.5 eV. In the spectrum analysis, the background signal was subtracted by Shirley's method.

2.3. Calculations

Quantum-chemical calculations were carried out using the three-parameter hybrid functional of Becke^[18] and Lee-Yang-Parr correlation functional^[19] (B3LYP method) included in the Jaguar package.^[20] Atomic orbitals were described by the 6-31G* basis

set. The CNT surface was modeled by a segment of an armchair (10,10) tube C₉₆H₂₄. Central part of the segment surface was decorated with fluorine atoms. Positions of carbon and hydrogen atoms at the segment edges were frozen during optimization, which was conducted using an analytical method to the gradient of $5 \cdot 10^{-4}$ atomic units for atom displacements.

Theoretical NEXAFS F K-spectra were constructed within the (Z + 1) approximation,^[21] which accounted for the effect of a final core hole created in the absorption process on the spectral profile. To model a core hole, the exciting fluorine atom (Z) was replaced by neon atom (Z + 1). For compensation of the extra valence electron, the calculating system was charged positively. Intensities of spectral lines were obtained by summing the squared coefficients at Ne 2p orbitals and broadened with Lorentzian functions of a width of 0.7 eV. X-ray transition energies were determined as a difference between Kohn-Sham eigenvalues of virtual molecular orbitals of a model calculated within the (Z + 1) approximation (excited system) and the 1s-level energy of fluorine in the ground state of that model. In such calculations, we use the energy of doubly occupied level instead of the energy of the F 1s level with a hole. This introduces a difference of ≈ 21 eV relative to the measured energies as it has been found from the comparison of the experimental F K-edge spectrum of graphite fluoride (CF)_n and theoretical spectrum^[22] obtained using the approach described above. This difference was used to correct the theoretical energy scale.

3. Results and Discussion

HRTEM images of the products detected the preservation of tubular structure of DWCNTs after fluorination at different conditions (**Figure 1**). The bundles of DWCNTs with an average size of ≈ 20 nm did not change their size after the fluorination at room temperature and decreased by half after the high-temperature fluorination. The interlayer separation in the fluorinated DWCNTs is close to 0.34 nm. However, the images

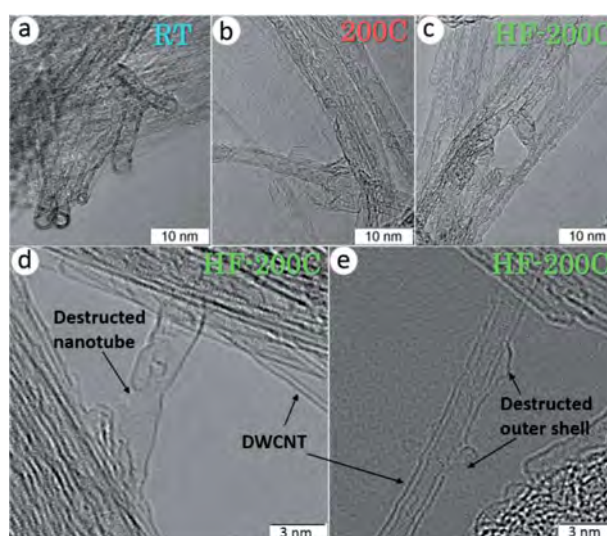


Figure 1. HRTEM images of DWCNTs fluorinated by pure F₂ at room temperature (a) and 200 °C (b) and F₂ in the presence of HF at 200 °C (c–e).

of the sample HF-200C obtained with a higher magnification display that some outer layers of DWCNTs are partially destructed and disoriented (Figure 1d,e).

To reveal the fluorination of the inner DWCNT shells, we have invoked the Raman spectroscopy. Figure 2 shows the Raman spectra measured in the region of radial breathing modes (RBM) from 100 to 300 cm^{-1} , corresponding to symmetric radial vibrations of carbon atoms, and in the region of D- and G-modes. In the spectrum of initial DWCNTs, the D-mode peak centered at 1324 cm^{-1} is a defect-activated feature, and G-mode peak at 1588 cm^{-1} appears owing to tangential in-plane stretching vibrations.^[23] Low intensity of D-mode peak indicates a high crystallinity of DWCNTs and low concentration of amorphous carbon in the purified sample. According to the relations $\omega_{\text{RBM}}(\text{cm}^{-1}) = 228/d(\text{nm})$ for inner tubes, and $\omega_{\text{RBM}}(\text{cm}^{-1}) = 204/d(\text{nm}) + 27(\text{cm}^{-1})$ for outer tubes, where d is a nanotube diameter, we detected responses from the inner shells with diameters of 0.9, 1.0, and 1.2 nm and from the outer shells with diameters of 1.4, 1.6, and 1.76 nm.^[24] As compared to initial DWCNTs, the Raman spectra of fluorinated DWCNTs showed suppressing the RBMs below 180 cm^{-1} (outer shells), while intensities of RBM peaks from the inner shells did not change significantly. The G-modes in the spectra of the fluorinated DWCNTs have different shapes and are slightly downshifted relative to the peak position for initial DWCNTs. The intensity of D-mode peak increased after the fluorination of DWCNTs. This peak is relatively weak in the spectrum of sample fluorinated at room temperature indicating a low amount of the attached fluorine. The largest intensity of D-mode peak for the DWCNTs fluorinated by F_2 -HF at 200 °C points at a high disordering of graphitic shells in this sample.

Figure 3 shows XPS C 1s and F 1s spectra of initial and fluorinated DWCNTs measured at an excitation energy of 800 eV. The XPS C 1s spectrum of pristine DWCNTs has a single asymmetric peak at 284.5 eV characteristic of sp^2 -graphitic carbon (peak C). The spectrum of DWCNTs fluorinated at room temperature exhibits new peaks centered at 285.4, 288.4, and 290.6 eV and attributed to carbon atoms linked with CF-groups (C-CF) and carbon atoms covalently bonded with one (C-F) and two (C-F₂) fluorine atoms, respectively. In the spectra of DWCNTs fluorinated at 200 °C, these additional peaks have the enhanced intensity, and they are shifted to higher energies to 286.1 eV (C-CF), 289.0 eV (CF), and 291.0 eV (CF₂). The fitting of the spectra by

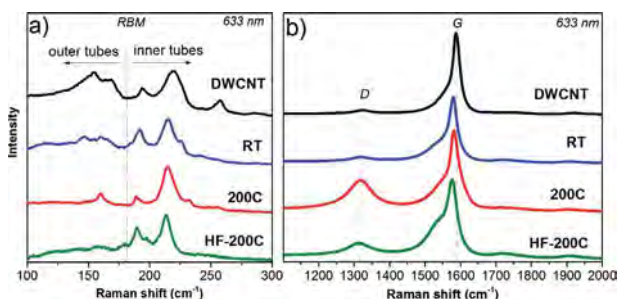


Figure 2. Raman spectra of initial DWCNTs and those after fluorination by pure F_2 at room temperature (RT) and 200 °C (200C) and by F_2 in the presence of HF at 200 °C (HF-200C) in RBM (a) and D- and G-mode (b) regions.

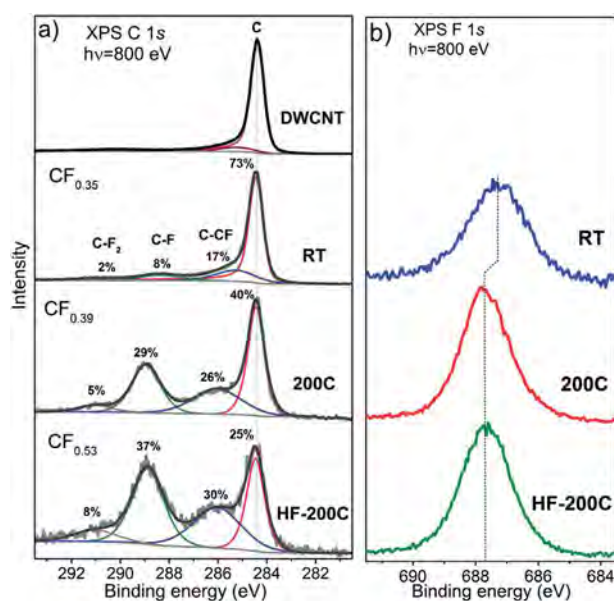


Figure 3. XPS spectra of initial DWCNTs and DWCNTs fluorinated by pure F_2 at room temperature (RT) and 200 °C (200C) and F_2 in the presence of HF at 200 °C (HF-200C) measured in the C 1s (a) and F 1s (b) regions at 800 eV.

components gave the compositions $\text{C}_{0.9}(\text{CF})_{0.08}(\text{CF}_2)_{0.02}$ for sample RT, $\text{C}_{0.66}(\text{CF})_{0.29}(\text{CF}_2)_{0.05}$ for sample 200C, and $\text{C}_{0.54}(\text{CF})_{0.37}(\text{CF}_2)_{0.08}$ for sample HF-200C.

Previously it has been demonstrated, that an increase of the fluorination temperature enhances the fluorination level of CNTs.^[4,7] According to the TEM and XPS characterizations, fluorination of MWCNTs by F_2/N_2 mixture at elevated temperatures 380, 420, and 450 °C caused the destruction of the tubular structure, disordering of graphene layers and formation of CF_2 groups mainly.^[25] We show that addition of HF in a F_2 flow allows obtaining the fluorinated DWCNTs with the higher fluorine loading for the shorter treatment period. A high concentration of CF_2 groups in the HF-200C sample is attributed to breaking of DWCNT layers because two fluorine atoms can be only bonded with an edge carbon atom. Since RBM signals from the inner shells are clearly observed in Raman spectra of the fluorinated DWCNTs, we assign the component C in their C1s spectra to these non-modified shells. Taking into account the diameters of the inner and the outer shells in the DWCNTs, we estimate 40% of interior carbon atoms.

Hence, in the case of fluorine attachment to the outer shells only, the area of the C component should be no less than 40% of the total spectrum area. The portion of this component determined from the XPS C1s spectra fitting is 59% for sample RT, 40% for sample 200C, and 24% for sample HF-200C. The reduced intensity of the component C for the last sample may indicate that inner shells of DWCNTs are partially fluorinated in this case. An average amount of carbon atoms adjacent to the CF-groups was estimated from a ratio of spectral areas of CF and C-CF components. The obtained values are 2.1 for sample RT, 0.9 for sample 200C, and 0.8 for sample HF-200C. In an ideal case, values 2 and 1 correspond to two and one bare (non-fluorinated) carbon atoms in a CF group surrounding. Thus, addition of HF

to F_2 should not change the fluorine pattern for DWCNTs fluorinated at $200^\circ C$.

This conclusion is supported by comparing the XPS F 1s spectra of the fluorinated DWCNTs (Figure 3b). The spectra are presented by a single symmetric peak located at 687.3 eV for the sample RT and 687.7 eV for the samples 200C and HF-200C. Previously it has been shown experimentally that the F 1s binding energy can increase with fluorine concentration and depends on fluorine pattern.^[7,22,26] The lower fluorine concentration and the weaker C–F interaction are observed for the DWCNTs fluorinated at room temperature, while the chemical state of fluorine is similar in both high-temperature fluorinated samples.

To study how the presence of HF in fluorine gas flow influences the ability of the F_2 molecules to penetrate inside the DWCNT bundles, the XPS C 1s spectra were measured at photon energies of 400, 800, and 1486.74 eV providing a sample probing depth of 0.44, 1.08, and 2.1 nm, respectively (Figure 4).^[27] The composition of the samples 200C and HF-200C estimated from the spectra fitting is $CF_{0.35}$ - $CF_{0.39}$ and $CF_{0.52}$ - $CF_{0.53}$, respectively. The ranges of the values show that fluorine is uniformly distributed within the bundles, independently on the presence or the absence of HF in the reaction volume. This observation is in contrast to that observed in Ref. [28], where the XPS C 1s spectra of MWCNTs fluorinated by a F_2 -HF mixture at $420^\circ C$ have detected an increase of the fluorinated carbon with probing depth.

The main difference between the C 1s spectra recorded at different excitation energies is a ratio between intensities of the components C–CF and C–F (Figure 4). The value C–CF/C–F decreases from 0.9 to 0.7 for sample 200C and from 0.8 to 0.7 for sample HF-200C, when the energy increases from 400 and 800 to 1486.74 eV. This evidences the change in the local surrounding of CF groups for the bundle surface and the bundle depth of

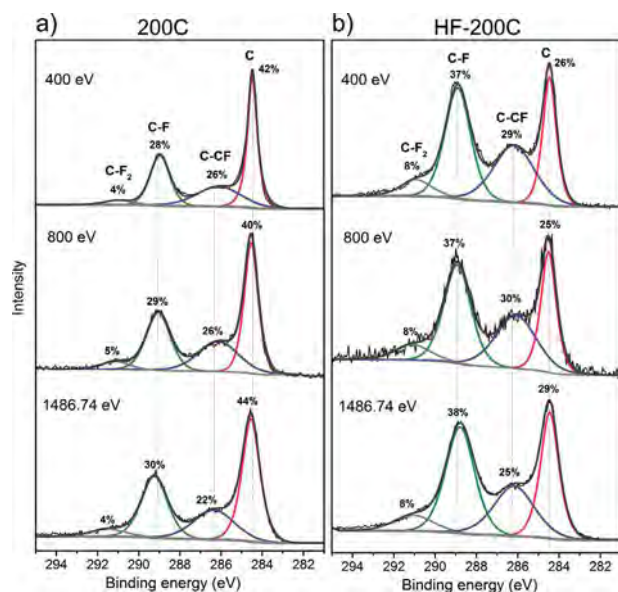


Figure 4. XPS C 1s spectra of DWCNTs fluorinated at $200^\circ C$ by pure F_2 (200C) and F_2 mixed with HF (HF-200C) measured at 400, 800, and 1486.74 eV.

2.1 nm. A reduced number of bare carbon atoms around a CF group should be attributed to the clustering of fluorine atoms inside the DWCNT bundles.

NEXAFS spectroscopy is a bulk sensitive method for nanostructured materials. Figure 5 compares the spectra measured near the C K- and F K-edges of the samples. The C K-edge spectrum of the initial DWCNTs exhibits intensive π^* - and σ^* - resonances at 285.4 and 291.8 eV, which are typical for graphite, carbon nanotubes and other structures with sp^2 -hybridized graphitic structure (Figure 5a). In the spectra of the fluorinated DWCNTs, intensity of the π^* -resonance is reduced and the σ^* -resonance has a smooth shape. Both these facts evidence changes in electronic structure of the DWCNTs as result of the fluorination. The spectral features located between 286.5 and 290.6 eV are contributed by carbon atoms covalently bonded with fluorine. The spectra of samples 200C and HF-200C are similar in appearance, while the spectrum of the sample RT shows higher π^* - and σ^* - resonances and weaker and localized peak C–F because of the lower fluorination degree and, probably, the different fluorine pattern.

The difference in the fluorine patterning for room-temperature and high-temperature fluorinated DWCNTs is detected from the NEXAFS F K-edge spectra. Before the σ^* - absorption edge at 692.2 eV, the spectrum of sample RT shows two shoulders A at 687.2 eV and B at 689.2 eV, while samples 200C and HF-200C have a single peak C at 688.3 eV (Figure 5b). The number, position, and intensity of pre-edge features are determined by the local surrounding of CF groups and depend

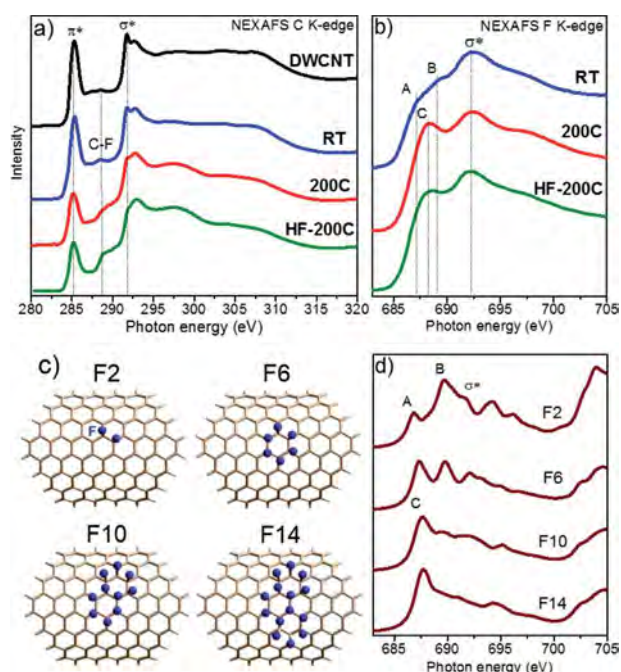


Figure 5. NEXAFS C K-edge spectra (a) and F K-edge spectra (b) of DWCNTs fluorinated by pure F_2 at RT and $200^\circ C$ and F_2 mixed with HF at $200^\circ C$. The optimized fragments of carbon nanotube (10, 10) $C_{96}H_{24}$ with two (F2), six (F6), ten (F10), and fourteen (F14) fluorine atoms (c). Theoretical F K-spectra calculated for all fluorine atoms in the models (d).

on the fluorination method.^[3] Note, that the pre-edge regions of F K-edge spectra of highly fluorinated MWCNTs as well as “white” graphite fluoride (CF)_n are dominated by a huge peak at the same position that the peak C in our case.^[28] The presence of highly fluorinated domains and inhomogeneous fluorine distribution were also observed in the SWCNTs fluorinated by pure F₂ gas.^[2]

To explain the main difference in the measured F K-edge spectra, four outer-surface fluorinated CNT models with different size of CF regions were considered (Figure 5c).

Two, six, ten, or fourteen fluorine atoms were attached to adjacent carbon atoms in the models F2, F6, F10, and F14. Theoretical F K-edge spectra constructed for all fluorine atoms in the models are compared in Figure 5d. The spectra of models F2 and F6 with small-size fluorinated regions exhibit two well-separated peaks in the pre-edge region, while the spectra of models F10 and F14 with larger CF-regions have a single pre-edge peak, which intensity increases with the size of the CF-region. An average number of bare carbon atoms adjacent to a CF group decreases from 2 to 0.7 in models F2 and F14. These numbers correlate with the values 2.1 and 0.8 experimentally determined for samples RT and HF-200C by the fitting the XPS C 1s spectra.

The experimental F K-edge spectrum of room-temperature fluorinated DWCNTs well matches with the spectra calculated for models F2 and F6, which show two pre-edge peaks A and B.

The F K-edge spectra of the DWCNTs fluorinated at 200 °C by pure F₂ and F₂ mixed with HF agree well with the spectra calculated for models F10 and F14. Thus, the direct fluorination of DWCNTs at high-temperature results in formation of small CF-areas, where fluorine atoms can be located on the surface side of outer shells. Due to repulsive electrostatic forces between fluorine atoms bonded to neighboring carbon atoms on the one side of a graphitic shell, the C–C bonds elongate and may break at the critical size of a CF area.^[29,8] Produced gaps in the outer DWCNT layers make the inner shells available for fluorination and the edged carbon atoms can attach two fluorine atoms with the formation of CF₂ groups, observed in the XPS C 1s spectra of our samples obtained at 200 °C (Figure 4).

In the present study, we have revealed that during fluorination by pure F₂ at room temperature only outer shells of DWCNTs are fluorinated. Fluorine pattern depends on the temperature of fluorination, pairs of fluorinated carbon are observed under mild conditions and small (CF)_n regions with fluorine atoms located at one-side of the outer shells of DWCNTs are developed at high temperature. A higher fluorination degree and partially fluorinated inner shells of DWCNTs were obtained at 200 °C in the presence of HF. Earlier, the fluorination of both inner and outer shells of DWCNTs was revealed when pure F₂ was used at 400 °C.^[30] By comparing the XPS and NEXAFS spectra of two DWCNT samples fluorinated by F₂ at 200 °C, we found no evidence that HF significantly influences the fluorine pattern. For the case of pure F₂, HF may also present on carbon surface due to the reaction of F₂ with a trace of adsorbed H₂O. The different fluorination kinetics of these samples may be explained by the amount of HF, *i.e.* as traces for F₂ and less than 5% for F₂–HF reactive atmosphere.

4. Conclusions

DWCNTs have been fluorinated by pure F₂ at room temperature for 3 h, at 200 °C for 2 h, and by F₂ mixed with HF at 200 °C for 10 min. The fluorination products were investigated by HRTEM, Raman spectroscopy, XPS, and NEXAFS. With the help of DFT modeling of NEXAFS F K-edge spectra, we found that increase of the fluorination temperature results not only in enhanced fluorine content but also in different fluorine patterns. Fluorine atoms covalently attach to pair or a few neighboring carbon atoms under room-temperature conditions, and to more than ten adjacent carbon atoms forming (CF)_n regions on outer sides of DWCNTs. The presence of HF in the fluorine gas significantly accelerates the process of DWCNT fluorination, but does not affect the fluorine pattern. The stoichiometry of CF_{0.53} achieved by DWCNT fluorination by F₂–HF at 200 °C was formed about 12 times faster than the composition of CF_{0.39} obtained using pure F₂ gas at the same temperature.

Acknowledgements

We thank Dr. B. A. Kolesov for the Raman spectra and Mr. A.V. Ischenko for the lower-magnified HRTEM images. The work has been financially supported by the Russian Foundation for Basic Research (Grant No. 16-53-150003) PRC CNRS/RFBR (Grant No. 1023) and the bilateral Program “Russian-German Laboratory at BESSY.”

Conflict of Interest

The authors declare no conflict of interest.

Keywords

double-walled carbon nanotubes, fluorination, HF, NEXAFS, X-ray photoelectron spectroscopy

- [1] K. N. Kudin, H. F. Bettinger, G. E. Scuseria, *Phys. Rev. B* **2001**, *63*, 045413.
- [2] W. Zhang, P. Bonnet, M. Dubois, C. P. Ewels, K. Guérin, E. Petit, J.-Y. Mevellec, L. Vidal, D. A. Ivanov, A. Hamwi, *Chem. Mater.* **2012**, *24*, 1744.
- [3] L. G. Bulusheva, Yu. V. Fedoseeva, A. V. Okotrub, E. Flahaut, I. P. Asanov, V. O. Koroteev, A. Yaya, C. P. Ewels, A. L. Chuvilin, A. Felten, G. Van Lier, D. V. Vyalikh, *Chem. Mater.* **2010**, *22*, 4197.
- [4] E. T. Mickelson, C. B. Huffman, A. G. Rinzler, R. E. Smalley, R. H. Hauge, J. L. Margrave, *Chem. Phys. Lett.* **1998**, *296*, 188.
- [5] D. E. Palin, K. D. Wadsworth, *Nature* **1948**, *162*, 925.
- [6] W. Feng, P. Long, Y. Feng, Y. Li, *Adv. Sci.* **2016**, *3*, 1500413.
- [7] K. H. An, J. G. Heo, K. G. Jeon, D. J. Bae, C. Jo, C. W. Yang, C.-Y. Park, Y. H. Lee, Y. S. Lee, Y. S. Chung, *Appl. Phys. Lett.* **2002**, *80*, 4235.
- [8] F. Chamssedine, D. Claves, *Chem. Phys. Lett.* **2008**, *454*, 252.
- [9] T. Mallouk, N. Bartlett, *J. Chem. Soc.: Chem. Commun.* **1983**, *3*, 103.
- [10] T. Mallouk, B. L. Hawkins, M. P. Conrad, K. Zilm, G. E. Maciel, N. Bartlett, *Philos. Trans. R. Soc. Lond. A* **1985**, *314*, 179.

- [11] F. Okino, H. Tanaka, P. Lagassie, S. Suganuma, H. Touhara, *J. Fluor. Chem.* **1992**, *57*, 45.
- [12] H. Muramatsu, Y. A. Kim, T. Hayashi, M. Endo, A. Yonemoto, H. Arikai, F. Okino, H. Touhara, *Chem. Commun.* **2005**, *15*, 2002.
- [13] T. Hayashi, D. Shimamoto, Y. Ahm Kim, H. Muramatsu, F. Okino, H. Touhara, T. Shimada, Y. Miyauchi, S. Maruyama, M. Terrones, M. S. Dresselhaus, M. Endo, *ACS Nano* **2008**, *2*, 485.
- [14] J. H. Kang, D. Takhar, O. V. Kuznetsov, V. N. Khabashesku, K. F. Kelly, *Chem. Phys. Lett.* **2012**, *534*, 43.
- [15] E. Flahaut, R. Bacsa, A. Peigney, C. Laurent, *Chem. Commun.* **2003**, *12*, 1442.
- [16] S. Osswald, E. Flahaut, Y. Gogotsi, *Chem. Mater.* **2006**, *18*, 1525.
- [17] S. Joachim, *NEXAFS Spectroscopy*, Springer, Berlin **1992**.
- [18] A. D. Becke, *J. Chem. Phys.* **1993**, *98*, 5648.
- [19] C. Lee, W. Yang, R. G. Parr, *Phys. Rev. B* **1988**, *37*, 785.
- [20] Jaguar software, version 9.2, Schrödinger LLC, New York, NY **2016**.
- [21] W. H. E. Schwarz, *Chem. Phys.* **1975**, *11*, 217.
- [22] L. G. Bulusheva, Yu. V. Fedoseeva, E. Flahaut, J. Rio, C. P. Ewels, V. O. Koroteev, G. Van Lier, D. V. Vyalikh, A. V. Okotrub, *Beilstein J. Nanotechnol.* **2017**, *8*, 1688.
- [23] M. S. Dresselhaus, G. Dresselhaus, A. Jorio, A. G. Souza, R. Saito, *Carbon* **2002**, *40*, 2043.
- [24] D. Levshov, T. X. Than, R. Arenal, V. N. Popov, R. Parret, M. Paillet, V. Jourdain, A. A. Zahab, T. Michel, Yu. I. Yuzyuk, J.-L. Sauvajol, *Nano Lett.* **2011**, *11*, 4800.
- [25] Y. Li, Y. Feng, W. Feng, *Electrochim. Acta* **2013**, *107*, 343.
- [26] M.-K. Seo, S.-J. Park, *Bull. Korean Chem. Soc.* **2009**, *30*, 2071.
- [27] S. Tanuma, C. J. Powell, D. R. Penn, *Surf. Interface Anal.* **2005**, *37*, 1.
- [28] M. M. Brzhezinskaya, V. E. Muradyan, N. A. Vinogradov, A. B. Preobrajenski, W. Gudat, A. S. Vinogradov, *Phys. Rev. B* **2009**, *79*, 155439.
- [29] M. Wu, J. S. Tse, J. Z. Jiang, *J. Phys. Chem. Lett.* **2010**, *1*, 1394.
- [30] H. Muramatsu, K. Fujisawa, Y.-I. Ko, K.-S. Yang, T. Hayashi, M. Endo, C.-M. Yang, Y. C. Jung, Y. A. Kim, *Chin. J. Catal.* **2014**, *35*, 864.